

# Observation of a dewetting transition in the collapse of the melittin tetramer

Pu Liu<sup>1</sup>, Xuhui Huang<sup>1</sup>, Ruhong Zhou<sup>1,2</sup> & B. J. Berne<sup>1,2</sup>

Marked hydration changes occur during the self-assembly of the melittin protein tetramer in water. Hydrophobicity induces a drying transition in the gap between simple sufficiently large (more than  $1\text{ nm}^2$ ) strongly hydrophobic surfaces as they approach each other<sup>1–6</sup>, resulting in the subsequent collapse of the system, as well as a depletion of water next to single surfaces<sup>7–10</sup>. Here we investigate whether the hydrophobic induced collapse of multidomain proteins or the formation of protein oligomers exhibits a similar drying transition. We performed computer simulations to study the collapse of the tetramer of melittin in water, and observed a marked water drying transition inside a nanoscale channel of the tetramer (with a channel size of up to two or three water-molecule diameters). This transition, although occurring on a microscopic length scale, is analogous to a first-order phase transition from liquid to vapour. We find that this drying is very sensitive to single mutations of the three isoleucines to less hydrophobic residues and that such mutations in the right locations can switch the channel from being dry to being wet. Thus, quite subtle changes in hydrophobic surface topology can profoundly influence the drying transition. We show that, even in the presence of the polar protein backbone, sufficiently hydrophobic protein surfaces can induce a liquid–vapour transition providing an enormous driving force towards further collapse. This behaviour was unexpected because of the absence of drying in the collapse of the multidomain protein 2,3-dihydroxybiphenyl dioxygenase (BphC).

Proteins exert electrostatic forces on water and are therefore much more complicated than purely hydrophobic systems. We have seen previously that because of these electrostatic forces there was no strong drying transition in the collapse of the BphC enzyme<sup>11</sup>, a two-domain protein. These findings showed that realistic protein–water forces have a significant function in hydrophobic collapse, and argued against a drying-induced reorganization model of protein folding. Others have examined the role of water during protein folding, finding that water can persist inside the core even after it collapses and can also act as a lubricant for folding<sup>12,13</sup>, but those studies did not address the drying transition that we discuss here. A coarse-grained simulation of the collapse of a model hydrophobic polymer chain showing that the evaporation (drying) of water in the vicinity of the polymer provides the driving force for the collapse, and that the rate-limiting step is the nucleation of a sufficiently large bubble, caused its authors<sup>14</sup> to speculate, “Our findings would seem also pertinent to the mechanism of biological assembly, such as protein folding, but to demonstrate so with simulation will require an analogous simulation study of a protein-like chain”. Here we study the water drying transition inside the melittin tetramer. Melittin, a 26-residue polypeptide, is a small toxic protein found in honeybee venom, which often self-assembles into a tetramer. Previous simu-

lations of hydration structure around the melittin dimer partly guided our choice of the tetramer for study<sup>15</sup>. The two dimers of the melittin tetramer are separated by a certain distance to create a nanoscale water ‘channel’. The enlarged melittin tetramer is then simulated with molecular dynamics. A strong, cooperative water drying transition is found inside the nanoscale channel whose size is large enough to encompass two or three water-molecule diameters, in agreement with previous speculation<sup>14</sup>.

For each enlarged melittin tetramer configuration (see Methods), three different types of molecular dynamics simulation were performed<sup>11</sup>: a ‘dewetting’ simulation starting with wet initial conditions (the channel filled with water molecules, protein atoms constrained); a ‘wetting’ simulation starting with dry initial conditions (no water molecules in the channel, protein atoms constrained); and a normal ‘folding’ simulation. In both the ‘dewetting’ and ‘wetting’ simulations, the protein atoms are constrained with a harmonic potential with a force constant of  $10\text{ kJ mol}^{-1}\text{ \AA}^{-2}$ , but water molecules and ions are free to move. For the ‘wetting’ simulation, the water molecules inside the tetramer channel are removed after equilibration. Figure 1a shows snapshots from one such ‘dewetting’ simulation with an initial separation distance  $D$  of  $5.5\text{ \AA}$ . A water vapour bubble developed very quickly, within about 100 ps, which fluctuated for a short period before growing to such a large size that all the water molecules inside the channel were expelled. The entire drying process took only about 300–400 ps in this case. Figure 1b shows a plot of the number of water molecules inside the channel compared with the molecular dynamics time for both ‘dewetting’ and ‘wetting’ simulations. The two water number curves converge after about 400 ps, and at the end no water molecules are observed near the centre of the nanoscale channel. These results clearly indicate that there is a strong water drying transition inside this nanoscale melittin tetramer channel. Other trajectories starting from different initial configurations show similar results (Supplementary Information). Careful simulations with many other separation distances show that the drying transition critical distance  $D_c$  for this melittin tetramer system is about  $5.5\text{--}7.0\text{ \AA}$ , which is equivalent to two or three water-molecule diameters.

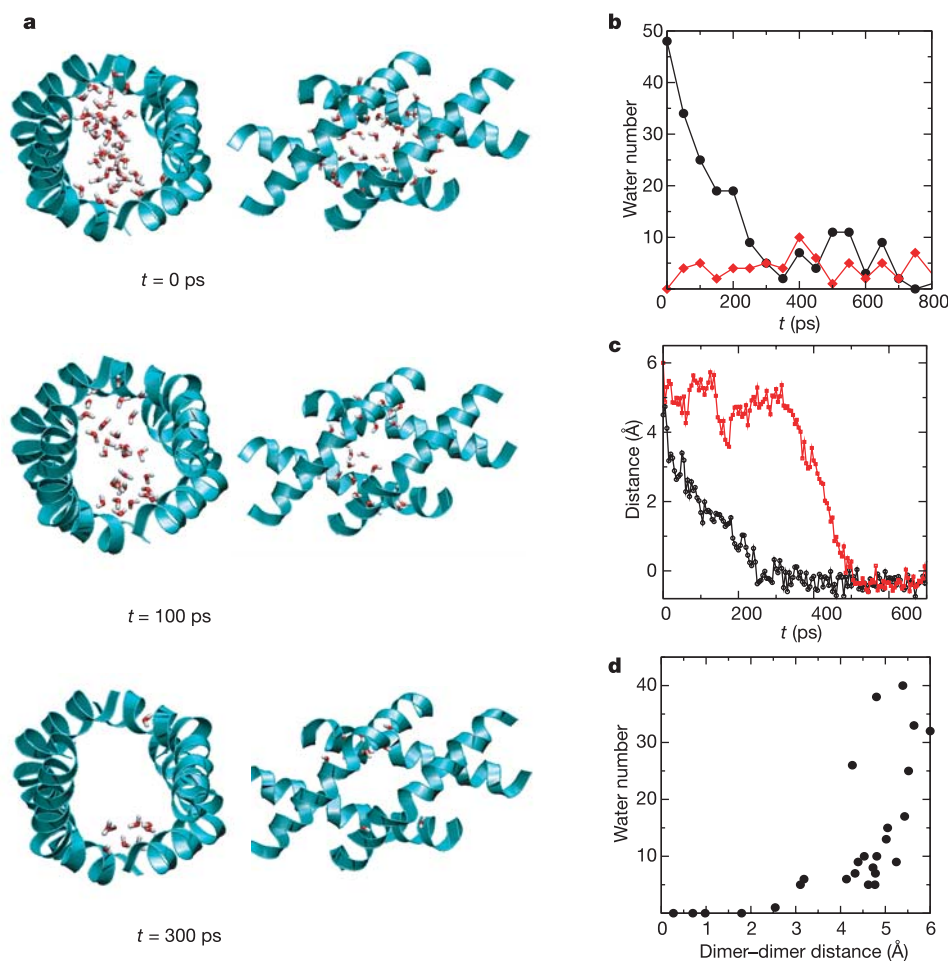
The kinetics of the collapse of the tetramer from its expanded configuration shows a very fast hydrophobic collapse when the two dimers are within the critical distance. Figure 1c plots a few trajectories of the dimer separation distance against the molecular dynamics time, starting from two different initial distances. The collapse can be very fast (as little as 150 ps) once it has passed through the initial diffusive stage. The collapse will be even faster, within 50 ps, if started from initial ‘dry’ condition. Large driving forces seem to be pushing the tetramers together, as recently observed in simulations of the collapse of paraffin-like plates where the collapse was found to be rate-limited by the nucleation of a vapour bubble in

<sup>1</sup>Department of Chemistry, Columbia University, New York, New York 10027, USA. <sup>2</sup>Computational Biology Center, IBM Thomas J. Watson Research Center, 1101 Kitchawan Road, Yorktown Heights, New York 10598, USA.

the gap<sup>5,8,9</sup>. A drying-induced collapse is found in some trajectories (one of them is shown in Fig. 1d), even though other trajectories show that drying and collapse happen at roughly the same time.

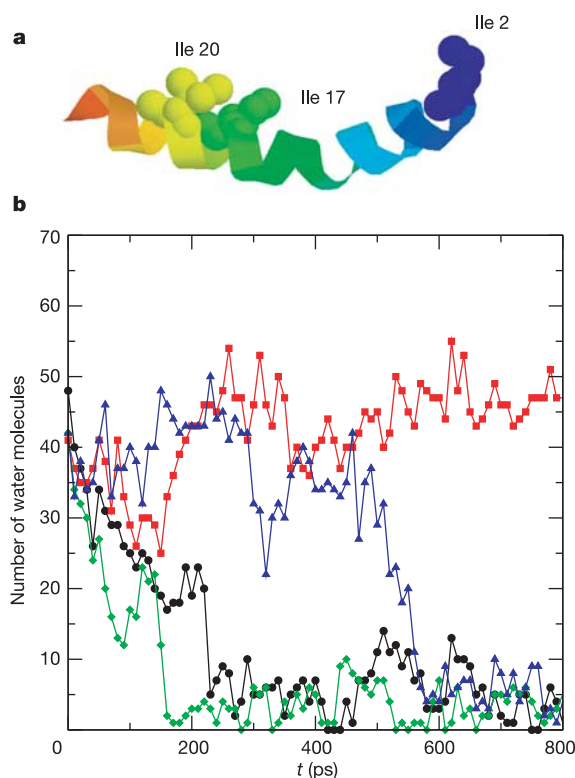
What makes this melittin tetramer behave differently from the BphC enzyme, the two-domain protein previously studied<sup>11</sup>? Even though BphC was chosen because it was thought to contain very hydrophobic domains based on a hydrophobic moment profile analysis, we did not find a water drying transition even at very small domain separations such as  $D = 4 \text{ \AA}$  (ref. 11). A quick analysis of the residue composition shows that the melittin tetramer is indeed very special—it has a very strong hydrophobic presence in the inner surface of the tetramer, with three Ile, four Leu, one Trp and two Val residues on each monomer helix. Meanwhile, it has five charged residues (three Lys and two Arg) on each monomer helix pointing away from the centre of the tetramer. It is therefore of great interest to see how sensitive the drying transition is to mutations of some of the key hydrophobic residues. We chose to perform single mutations of the Ile residues, which are the most hydrophobic residues on melittin. The locations of Ile 2, Ile 17 and Ile 20 are shown in Fig. 2a. Three different types of mutation were performed, Ile to Val, Ile to Ala, and Ile to Gly, with decreasing hydrophobicity. All these mutations were single mutations; in other words, only one Ile residue was mutated at any time for each monomer.

Table 1 summarizes the effects of the mutations. As expected, single mutations to Gly have the strongest effect and mutations to Val have the least effect. In addition, for Gly mutations, significantly different results can happen depending on the mutation location: Ile2Gly wets, Ile17Gly dries (dewets), and Ile20Gly fluctuates between wet and dry. In contrast, the effects of mutations to Ala fall somewhere between. Figure 2b shows a plot of the number of water molecules inside the tetramer channel against the molecular dynamics simulation time for all three Ala mutations (see Supplementary Information for more trajectories). The Ile17Ala mutation (green curve) still shows a sharp drying transition, with water density inside the channel decreasing to zero after about 200 ps. However, the Ile2Ala mutation (red curve) shows no drying transition during the entire simulation. The Ile20Ala mutation (blue curve) leads to larger fluctuations in water density and dewets noticeably more slowly (after 600 ps). The most interesting finding from Table 1, however, is that Ile 2 seems to be the most sensitive residue: all three single mutations at that position cause the water drying transition to disappear. Considering that Val is also a very hydrophobic residue, the Ile 2 position is indeed very sensitive to mutations. A closer look shows that residue Ile 2 protrudes from the dimer plane, acting as a ‘bump’ or ‘door’ to the tetramer channel (see Fig. 3a). The Ile 20 residue also shows a bump, but not as large as that



**Figure 1 | Dewetting in melittin.** **a**, Snapshots of water molecules inside the gap of the melittin tetramer (the protein is shown as ribbons and water as sticks). Only water molecules near the centre of the channel are plotted, which is defined as the region with a spherical radius of  $10 \text{ \AA}$  from the centre of the enlarged tetramer. **b**, Plot of the number of water molecules inside the channel against the molecular dynamics time for ‘dewetting’ (black) and ‘wetting’ (red) simulations. **c**, The kinetics of the ‘folding’ simulation

starting from two different initial separations,  $D = 6 \text{ \AA}$  (black) and  $D = 4.5 \text{ \AA}$  (red). **d**, Plot of the number of water molecules inside the channel against the dimer-dimer distance for one folding trajectory starting at an initial separation of  $6 \text{ \AA}$ , which indicates a drying-induced collapse (see Supplementary Information for more trajectories showing drying and collapse happening at roughly the same time).



**Figure 2 | Dewetting in mutated melittin.** **a**, Illustration of three mutation sites, Ile 2, Ile 17 and Ile 20, on one monomer. Ile 2 is sticking out the dimer plane, and Ile 17 is lying on the plane; Ile 20 is somewhat tilted, with a conformation between those of Ile 2 and Ile 17. **b**, The number of water molecules in the tetramer channel with  $D = 5.5 \text{ \AA}$  as a function of simulation time. It is clear that the dewetting strength is sensitive to the surface topology of the protein. Black, no mutation; red, Ile2Ala; green, Ile17Ala; blue, Ile20Ala.

for Ile 2, whereas Ile 17 lies on the dimer plane. This special surface topology might be responsible for Ile2's central role in the drying transition in this melittin tetramer.

To improve our understanding of the function of the Ile 2 residue in surface topology, we designed a model system to mimic the shape

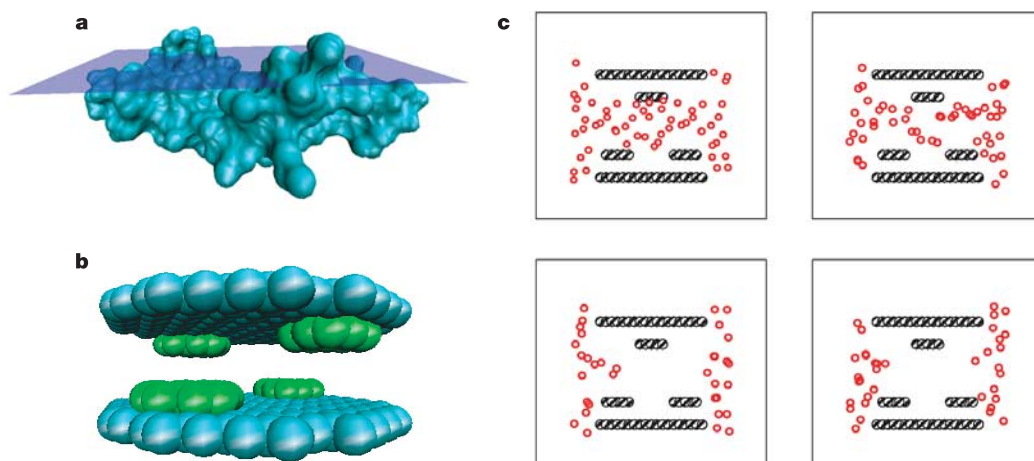


**Figure 3 | Dewetting in a model system.** **a**, The topology of a melittin dimer. The reference plane shows two bumps in the region between two dimers. **b**, A model system of two graphite-like plates with two argon 'bumps' (green balls)

**Table 1 | Dewetting results from single mutations on three Ile residues of each melittin monomer**

Model	Ile 2	Ile 17	Ile 20
No mutation	Dewet	Dewet	Dewet
Mutate to Val	Wet	Dewet	Dewet
Mutate to Ala	Wet	Dewet	Dewet
Mutate to Gly	Wet	Dewet	Fluctuation

characteristics of the melittin tetramer. Figure 3b shows a model of two graphite-like plate systems. Two argon clusters were grown to mimic the surface bumps on the graphite surface. Each graphite-like plate has 170 carbon atoms with C–C Lennard–Jones interaction reduced to  $\epsilon_{cc} = 0.0213 \text{ kcal mol}^{-1}$  (for comparison,  $\epsilon_{cc}$  for graphite is  $0.0860 \text{ kcal mol}^{-1}$ ). This results in a plate with a radius of about  $14 \text{ \AA}$ . Each argon cluster has 13 argon atoms (with  $\epsilon = 0.00656 \text{ kcal mol}^{-1}$ ) and the distance from each argon atom to the nearest surface carbon atom is about  $2.2 \text{ \AA}$ . For this graphite-like plate system, the critical distance is  $4.5\text{--}6.5 \text{ \AA}$  (measured from one plate surface to the other plate surface) without the bumps, and it increases to about  $6.5\text{--}8.5 \text{ \AA}$  with the bumps. Thus, these argon cluster bumps have increased the transition critical distance by about  $2 \text{ \AA}$ . These surface bumps disrupt the hydrogen-bond network of water between the plates, thus making the wet configurations less favourable. This disruption is probably even more extensive for the tetramer channel, given its greater surface irregularity. The water hydrogen-bond network is energetically more critical in the tetramer channel case than the two-plate case, because the channel is one-dimension-like whereas the inter-plate region is two-dimensional.

There seem to be two reasons why the melittin tetramer channel shows a drying transition while the two-domain protein BphC does not. The melittin channel is like a tube, whereas the inter-domain region in the two-domain protein is a slab. It is less costly in terms of free energy to disrupt the hydrogen bonds in a tube-like channel. Moreover, the special surface topology springing from the Ile residues destabilizes the wetting in the channel. Even though there has been no direct experimental evidence yet for this nanoscale dewetting transition in real proteins, two recent experiments have shown partial dewetting for paraffin-like systems<sup>1,16,17</sup>: one for  $^2\text{H}_2\text{O}$  in contact with deuterated polystyrene in a neutron reflectivity experiment<sup>16</sup>, and the other using water in contact with paraffin in an X-ray reflectivity experiment<sup>17</sup>. Partial dewetting was found, with a water density about 10% lower than the bulk near the interface. It would be of interest to devise experiments to test our predictions above for melittin tetramers.

on each plate. **c**, Snapshots of drying transition as a function of time for this model plate system embedded in Simple Point Charge (SPC) water (only oxygen atoms of water are shown; red dots). The inter-plate distance is  $6.5 \text{ \AA}$ .

Previous work<sup>3,6</sup> has shown that drying is very sensitive to very small changes in the attractive interactions between hydrophobic particles and water. Our results, showing that drying is exquisitely sensitive to point mutations of Ile to less hydrophobic residues, are consistent with those studies, and demonstrate that in special cases the self-assembly or collapse of proteins can be induced by the evaporation of water (drying) in regions enclosed by their hydrophobic surfaces.

## METHODS

The starting structure of the melittin tetramer is taken from the crystal structure deposited in PDB (accession number 2mlt.pdb)<sup>18</sup>. The two dimers (chains A and B, and chains C and D) of the tetramer are separated by a distance  $D$ , ranging from 4.0 to 8.0 Å, to create a 'nanoscale channel', and are then solvated in water boxes with water molecules at least 8 Å from the protein surface. Twenty Cl<sup>-</sup> counterions are added to all solvated water boxes to make the system electrically neutral. The final solvated protein systems have up to 25,000 atoms (the actual size varies for different channel sizes  $D$ ). The OPLSAA force field is used for the protein<sup>19</sup> and the SPC water model for the explicit solvent, with a cut-off of 12 Å for the non-bonded interactions. The GROMACS simulation package is used here for this large system because of its fast speed<sup>20</sup>. Constant-pressure, constant-temperature (normal pressure and temperature: 1 atm and 300 K) molecular dynamics with a time step of 1.0 fs is used for each system after a conjugate gradient minimization. A total of ten different 'proteins', one native and nine single mutations (each of the three Ile residues mutated to Val, Ala and Gly, respectively), are simulated starting at five different initial separations ( $D = 4$  to 8 Å), with up to ten different initial configurations for each separation (same protein conformer but solvated in different water boxes) and up to 10 ns of molecular dynamics simulation, which aggregates to more than 1 μs of total molecular dynamics time. Some of the simulations were run on IBM BlueGene/L development machines.

Received 18 February; accepted 19 June 2005.

- Ball, P. How to keep dry in water. *Nature* **423**, 25–26 (2003).
- Wallqvist, A. & Berne, B. J. Computer simulation of hydrophobic hydration forces on stacked plates at short range. *J. Phys. Chem.* **99**, 2893–2899 (1995).
- Hummer, G., Rasaiah, J. R. & Noworyta, J. P. Water conduction through the hydrophobic channel of a carbon nanotube. *Nature* **414**, 188–190 (2001).
- Leung, K., Luzar, A. & Bratko, D. Dynamics of capillary drying in water. *Phys. Rev. Lett.* **90**, 065502 (2003).
- Huang, X., Margulis, C. J. & Berne, B. J. The dewetting and collapse of nanoscale hydrophobic objects. *Proc. Natl Acad. Sci. USA* **100**, 11953–11958 (2003).
- Huang, X., Zhou, R. & Berne, B. J. Drying and hydrophobic collapse of paraffin plates. *J. Phys. Chem. B* **109**, 3546–3552 (2005).
- Stillinger, F. H. Structure in aqueous solutions of nonpolar solutes from the standpoint of scaled-particle theory. *J. Solution Chem.* **2**, 141–158 (1973).
- Lum, K., Chandler, D. & Weeks, J. D. Hydrophobicity at small and large length scales. *J. Phys. Chem. B* **103**, 4570–4577 (1999).
- Chandler, D. Two faces of water. *Nature* **417**, 491 (2002).
- Sansom, M. S. P. & Biggin, P. C. Biophysics: water at the nanoscale. *Nature* **414**, 156–159 (2001).
- Zhou, R., Huang, X., Margulius, C. J. & Berne, B. J. Hydrophobic collapse in multidomain protein folding. *Science* **305**, 1605–1609 (2004).
- Shea, J., Onuchic, J. & Brooks, C. L. Probing the folding free energy landscape of the src-SH3 protein domain. *Proc. Natl Acad. Sci. USA* **99**, 16064–16068 (2002).
- Cheung, M. S., Garcia, A. E. & Onuchic, J. Protein folding mediated by solvation: water expulsion and formation of the hydrophobic core occur after the structural collapse. *Proc. Natl Acad. Sci. USA* **99**, 685–690 (2002).
- Wolde, P. R. T. & Chandler, D. Drying-induced hydrophobic polymer collapse. *Proc. Natl Acad. Sci. USA* **99**, 6539–6543 (2002).
- Cheng, Y. & Rossky, P. J. Surface topography dependence of biomolecular hydrophobic hydration. *Nature* **392**, 696–699 (1998).
- Steitz, R. *et al.* Nanobubbles and their precursor layer at the interface of water against a hydrophobic substrate. *Langmuir* **19**, 2409–2418 (2003).
- Jensen, T. R. *et al.* Water in contact with extended hydrophobic surfaces: Direct evidence of weak dewetting. *Phys. Rev. Lett.* **90**, 086101 (2003).
- Terwilliger, T. C. & Eisenberg, D. The structure of melittin. *J. Biol. Chem.* **257**, 6010–6015 (1982).
- Jorgensen, W. L., Maxwell, D. & Tirado-Rives, J. Development and testing of the OPLS all-atom force field on conformational energetics and properties of organic liquids. *J. Am. Chem. Soc.* **118**, 11225–11236 (1996).
- Lindahl, E., Hess, B. & van der Spoel, D. Gromacs 3.0: A package for molecular simulation and trajectory analysis. *J. Mol. Model.* **7**, 306–317 (2001).

Supplementary Information is linked to the online version of the paper at [www.nature.com/nature](http://www.nature.com/nature).

**Acknowledgements** We thank J. Castanos and his team for providing the running environment, and M. Eleftheriou, B. Walkup and A. Royyuru for help and support with the BlueGene/L machine. This work was supported in part by an NIH grant and an IBM SUR grant to B.J.B.

**Author Information** Reprints and permissions information is available at [npg.nature.com/reprintsandpermissions](http://npg.nature.com/reprintsandpermissions). The authors declare no competing financial interests. Correspondence and requests for materials should be addressed to R.Z. ([ruhongz@us.ibm.com](mailto:ruhongz@us.ibm.com)) and B.J.B. ([berne@chem.columbia.edu](mailto:berne@chem.columbia.edu)).